



Published in final edited form as:

*J Comp Neurol.* 2009 May 20; 514(3): 272–283. doi:10.1002/cne.22019.

## Altered Cutaneous Nerve Regeneration in a Simian Immunodeficiency Virus/Macaque Intracutaneous Axotomy Model

Gigi J. Ebenezer<sup>1</sup>, Victoria A. Laast<sup>2</sup>, Brandon Dearman<sup>1</sup>, Peter Hauer<sup>1</sup>, Patrick M. Tarwater<sup>3</sup>, Robert J. Adams<sup>2</sup>, M. Christine Zink<sup>2,4</sup>, Justin C. McArthur<sup>1,4,5</sup>, and Joseph L. Mankowski<sup>1,2,4</sup>

<sup>1</sup>Department of Neurology, Johns Hopkins University, Baltimore, Maryland 21287-7609

<sup>2</sup>Department of Molecular and Comparative Pathobiology, Johns Hopkins University, Baltimore, MD 21287, USA

<sup>3</sup>Department of Biostatistics and Epidemiology, University of Texas Health Science Center at Houston, School of Public Health, El Paso Regional Campus, 1100 N. Stanton, Suite 110, El Paso, TX 79902

<sup>4</sup>Department of Pathology, Johns Hopkins University, Baltimore, Maryland 21287-7609

<sup>5</sup>Department of Epidemiology, Johns Hopkins University, Baltimore, Maryland 21287-7609

### Abstract

To characterize the regenerative pattern of cutaneous nerves in SIV-infected and uninfected macaques, excisional axotomies were performed in non-glabrous skin at 14-day intervals. Samples were examined after immunostaining for the pan-axonal marker PGP 9.5 and the Schwann cell marker p75 nerve growth factor receptor. Collateral sprouting of axons from adjacent uninjured superficial dermal nerve bundles was the initial response to axotomy. Both horizontal collateral sprouts and dense vertical regeneration of axons from the deeper dermis led to complete, rapid reinnervation of the epidermis at the axotomy site. In contrast to the slower, incomplete reinnervation previously noted in humans after this technique, in both SIV-infected and uninfected macaques, epidermal reinnervation was rapid and completed by 56 days post-axotomy. p75 was densely expressed on the Schwann cells of uninjured nerve bundles along the excision line and on epidermal Schwann cell processes. In both SIV-infected and uninfected macaques, Schwann cell process density was highest at the earliest time points post-axotomy and then declined at a similar rate. However, SIV-infection delayed epidermal nerve fiber regeneration and remodeling of new sprouts at every time point post-axotomy, and SIV-infected animals consistently had lower mean epidermal Schwann cell densities suggesting that Schwann cell guidance and support of epidermal nerve fiber regeneration may account for altered nerve regeneration. The relatively rapid regeneration time and the completeness of epidermal reinnervation in this macaque model provides a useful platform for assessing the efficacy of neurotrophic or regenerative drugs for sensory neuropathies including those caused by HIV, diabetes mellitus, medications, and toxins.

### Keywords

SIV; epidermal axons; Schwann cells; sprouting axon; p75; PGP9.5

## INTRODUCTION

Injury to the peripheral nervous system represents a major and growing source of disability (Dyck et al., 1993; Kar and Job, 2005; McArthur et al., 2005; Ownby and Dune, 2007; Ziegler et al., 1992). Human immunodeficiency virus -associated sensory neuropathy (HIV-SN) remains one of the most common neurologic complications of HIV infection with up to 35% of HIV-infected adults developing signs of HIV-associated sensory neuropathy (HIV-SN) (Cornblath and McArthur, 1988; Lichtenstein et al., 2005; So et al., 1988) with associated epidermal nerve fiber degeneration (Herrmann et al., 2004; Herrmann et al., 2006; Zhou et al., 2007). Because intraepidermal nerve fiber (IENF) evaluation in punch skin biopsies can detect subtle changes in epidermal innervation, IENF density measurement is an ideal surrogate marker of both nerve degeneration and regeneration including nerve damage caused by HIV infection (Gibbons et al., 2006; Hirai et al., 2000; Lauria et al., 2003; McArthur and Griffin, 2005; Polydefkis et al., 2004; Polydefkis et al., 2006; Polydefkis et al., 2002).

The SIV/pigtailed macaque model has proven to be an excellent animal model to investigate the pathogenic mechanisms of HIV infection including both HIV-induced CNS disease and damage to peripheral nervous system somatosensory ganglia (Clements et al., 2002; Haigwood, 2004; Laast et al., 2007; Mankowski et al., 2002a; Mankowski et al., 2004; Mankowski et al., 2002b; Van Rompay et al., 2006; Zink et al., 2001; Zink et al., 2006). In this model, pigtailed macaques are simultaneously inoculated with the neurovirulent recombinant SIV clone SIV/17E-Fr and the immunosuppressive swarm SIV/DeltaB670. In this report, we used this well-described SIV/macaque model to determine whether SIV infection altered cutaneous nerve regeneration following intracutaneous axotomy to further our understanding of the pathogenesis of lentiviral-induced sensory neuropathy.

Despite considerable research in the past decade, many questions in the field of peripheral nerve injury remain unanswered, particularly on how best to model nerve injury and probe the effects of drugs that may stimulate nerve repair. The mechanisms by which peripheral nerves reinnervate the skin have been studied in humans with two distinct patterns of reinnervation described: 1) regeneration of the injured nerve itself and 2) collateral sprouting from intact neighboring nerves. These patterns were observed in humans using an excision model that created a denervated area in the epidermis by removal of a cylindrical piece of skin. In healthy controls, complete reinnervation was not achieved in this excision model even after 23 months (Rajan et al., 2003).

In this study we used excision skin biopsies to accomplish two related goals: first, to characterize the intraepidermal reinnervation pattern after intracutaneous axotomy in a primate model to permit direct comparison with our previous parallel studies in humans and second, to determine whether SIV infection altered the course of intraepidermal nerve fiber repair in SIV-infected pig-tailed macaques.

## MATERIALS AND METHODS

### Animal studies

Six uninfected and five SIV-infected juvenile pig-tailed macaques (*Macaca nemestrina*) were used in this study. SIV-infected macaques were inoculated intravenously simultaneously with the neurovirulent clone SIV/17E-Fr and the immunosuppressive swarm SIV/DeltaB670 as previously described (Laast et al., 2007; Mankowski et al., 2002a; Mankowski et al., 2004; Mankowski et al., 2002b). Beginning 2 weeks post-SIV inoculation, 3 mm diameter cutaneous axotomies were performed at two-week intervals on

the dorsal interscapular skin of the back, 2 cm lateral to the spinous processes between T4 and T10. At each time point, a single incision was made using a 3 mm circular skin punch (Acuderm, Ft Lauderdale, FL) transecting epidermis and dermis to a depth of approximately 4 mm extending into the subcutaneous layer (Fig 1A). The chief purpose of these serial circular incisions was to uniformly transect epidermal axons to allow evaluation of epidermal nerve fiber re-growth back into the healing region of skin post-transection. Each incision was located 1 cm caudal to the previous site at the same distance from the dorsal midline. Excisional sites were allowed to heal without sutures or other interventions (Fig. 1B). On the 70th day after the initial incision, a 5 mm circular biopsy punch, overlapping the previous excision punch, was used to harvest all of the previous 3 mm punch sites, thereby yielding samples containing excision sites that were 14, 28, 42, 56 and 70 days post-axotomy (Fig. 1B; Fig. 2A). A separate 5 mm diameter control sample was obtained from normal skin remote from previous excisional axotomy sites to quantify normal Schwann cell density in each animal. To perform these procedures, macaques were anesthetized with 15 mg/kg ketamine administered intramuscularly. For euthanasia, pentobarbital was administered intravenously to effect. The animal procedures in this study were reviewed and approved by the institutional animal care and use committee in accordance with Animal Welfare Act regulations and the USPHS Policy on humane care and use of Laboratory Animals.

### Immunohistochemistry and immunofluorescence

Tissue samples were fixed in 2% paraformaldehyde/lysine/periodate (PLP) for 24 hours and processed for sectioning according to previously described techniques (Holland et al., 1997; McCarthy et al., 1995). The biopsies were sectioned with a sliding microtome into 50  $\mu$ M thick frozen vertical free-floating sections. The primary antibody used to detect nerve fibers was a rabbit anti-PGP 9.5 antibody (Chemicon, Temecula, CA; 1:2000 dilution). This antibody was generated using recombinant human ubiquitin C-terminal hydrolase (UCH-L1) as immunogen. This antibody recognizes a single 24 kDa band on Western blot of macaque nerve and the immunostaining pattern of epidermal nerve fibers in macaques is consistent with previous reports (McCarthy et al., 1995; Rajan et al., 2003; Wendelschafer-Crabb et al., 2006; Wilkinson et al., 1989). To label Schwann cells, antibody directed against the nerve growth factor- receptor p75 was used. This antibody was generated using the human melanoma cell line WM245 as immunogen. This antibody detects a single 75 kDa band on western blot of macaque nerve tissue and the immunostaining pattern obtained using this antibody in macaque tissue is consistent with other studies (Rajan et al., 2003; Ross et al., 1984). An antibody directed against the S-100  $\beta$ -subunit generated by using purified bovine s100b as immunogen (Clone SH-B4; Sigma, St. Louis, MO; 1:500 dilution) was also used to detect Schwann cells. This antibody recognizes a single band of approximately 10 kDa on Western blot of macaque nerve and the immunostaining pattern obtained using this antibody in macaque tissue is consistent with other studies (Baudier and Gerard, 1986; Donato, 2001). Table 1 contains additional specific details of these antibodies.

Nonspecific binding of secondary antibodies was blocked with 4% normal goat serum (NGS, 1.0% Triton X-100, 0.5% nonfat powdered milk in Tris-buffered saline (TBS), pH 7.4. Sections were rinsed in TBS, pH 7.4, and transferred to secondary antibodies. Secondary antibodies included goat anti-rabbit IgG (Vector Laboratories, Burlingame, CA) and goat anti-mouse IgG (Vector Laboratories, Burlingame, CA) that were used at 1:100 dilutions.

The sections were incubated with Avidin-Biotin Complex solution (Vector Laboratories, Burlingame, CA) and color was developed with chromogens. PGP 9.5 stained sections were developed with blue/gray (SG) chromophore and the p75 and s100 stained sections with diaminobenzidine (DAB). 1% Eosin and Mayer's hematoxylin were used as counterstains.

Primary antibodies were omitted and normal rabbit serum (1:2000; Vector Laboratories, Burlingame, CA), and mouse IgG (1:500; Vector Laboratories, Burlingame, CA) were used as negative controls for immunohistochemistry.

For studies using immunofluorescence, the secondary antibody Cy3 goat anti-rabbit IgG (Jackson Immuno Research Laboratories, Inc, West Grove, PA) was used at 1:150 dilution and Alexa-Fluor goat anti-mouse IgG (Invitrogen, Carlsbad, CA) at 1:500 dilution. After rinsing in TBS, the fluorescence-labeled sections were mounted in Mowiol 4–88 (Calbiochem, San Diego, CA) to prevent fluorescent quenching. DRAQ5 (Biostatus Ltd, San Diego, CA) was used for nuclear staining. Fluorescent samples were analyzed using a Zeiss LSM510 confocal imaging system. The images were collected in 1  $\mu$ m optical Z-series sections and reconstructed into a single image, as has been described previously for skin biopsies (Kennedy and Wendelschafer-Crabb, 1993; Rice and Rasmusson, 2000). Using Adobe Photoshop CS v. 8.0 Software (Adobe System, San Jose, CA) the photomicrographs were only adjusted for contrast and brightness levels for optimal quality and positioned into the montages.

### Morphometry

Epidermal nerve fiber length of 10 sprouting collateral epidermal fibers that extended into the excisional site from the edge of the axotomy site and 10 epidermal nerve fibers in the epidermis outside the axotomy site (Fig. 2B and Fig. 5A) were measured and documented using Bioquant 2.50.4 (Bioquant Life Sciences) under 400x magnification. The sprouting epidermal fibers (termed sprouts = S) reflected reinnervation into the excisional site denervated by the axotomy. The epidermal fibers outside the initial axotomy zone, (termed normal = N) represented normal epidermal fibers. By measuring both sprout and normal fiber lengths in each individual animal, we were able to determine the ratio of sprout length to normal fiber length for each animal, thereby controlling for variation in normal fiber length between animals. For measuring fiber lengths, epidermal nerve fiber length was defined as the length of the nerve fiber from basement membrane from entry point in the epidermis to the free terminal ending. Because the innervation in macaques is extremely dense, no technique has previously been validated in macaques to quantify epidermal nerve fiber density, in contradistinction to humans (Stocks et al., 1996).

To measure intra-epidermal Schwann cell process density, the number of p75-positive Schwann cell cytoplasmic processes that extended into the epidermis were counted in 5 mm diameter samples overlapping 3 mm excision sites as well as in the control skin (Fig 2.F). The length of the epidermis along the upper margin of the stratum corneum was measured with Bioquant software (R&M Biometrics, Nashville, TN). The Schwann cell process density was derived and expressed as the number of Schwann cell processes per millimeter of epidermal length (cells/mm) using the same counting rule as previously described for intraepidermal axons (Ebenezer et al., 2007a; Kennedy et al., 2005; Lauria et al., 2005; McArthur et al., 1998; Stocks et al., 1996).

### Statistical Analysis

Descriptive statistics for the ratio of sprouts:normal fibers (S:N ratio) and Schwann cell density in epidermis were calculated as mean and standard deviation for each group (i.e., uninfected and infected) at each observed day post-axotomy. Analysis of the change in fiber ratio and Schwann cell density over time utilized a linear regression model which yielded a mean rate of change over time, represented by the slope for each group, as well as the test statistics and p-value for the difference, if any, between the two rates. Since all data were not independent (i.e., each animal contributed multiple measurements over time) the regression model required use of repeated measures methodology which accounted for the correlation

inherent between measurements on the same subjects observed separately over time, thus producing appropriately adjusted standard error estimates.

## RESULTS

### Axonal regrowth

No epidermal or dermal axons were identifiable with PGP 9.5 immunostaining in the post-axotomy excision site at Day 14 (Fig. 2A). Subsequently, epidermal reinnervation occurred predominantly as a result of collateral sprouting. At the excision margin, at 28 days post-axotomy, the axons had sprouted from uninjured dermal nerve bundles and entered and elongated vertically within the supra-basal layers of epidermis. These axons were aligned in a slanting pattern within the epidermis (Fig. 2B). In addition to elongation of these axons in epidermis, collateral sprouts ensheathed by Schwann cells (Fig. 3 B2 and B3) formed thin nerve bundles that grew along the dermal-epidermal junction close to the basement membrane and reached the center of the denervated zone (Fig. 2B and D). These bundles coursing along the dermal-epidermal junction gave rise to numerous vertically oriented branches to produce intraepidermal axons that extended to the stratum corneum of the epidermis (Fig. 2C, Fig. 3A and B1). Throughout the course of regeneration, the collateral epidermal fibers at the excision margin tended to orient towards the center of the denervated zone. By 56 days post-axotomy, these inward-leaning sprouts appeared to retract, straighten (Fig. 2D), and then reach the height of the surrounding, uninjured epidermal axons. In the central denervated zone, by 42–56 days post-axotomy, the regenerating axons from the dermal plexus grew through the dermal collagen, vertically entered the epidermis, and completed the reinnervation process (Fig. 2C and D).

### Schwann cell regrowth

At Day 14 post-axotomy, p75-immunopositive transected Schwann cell bands were present in the dermis at the base of the excision site, lying flat and oriented parallel to the surface of the epidermis (Fig. 2E). By 28 days post-axotomy, p75 was densely expressed at the excision line along the uninjured nerve bundles (Fig. 3A). Schwann cell processes with collateral sprouting axons formed thin nerve bundles (Fig. 2F, Fig. 3B3) that extended horizontally towards the midline of the excision site along the dermal-epidermal junction, close to the basement membrane.

After reaching the central denervated zone of the dermis, the Schwann cell bands turned vertically towards the epidermis (perpendicular to the epidermal surface; Fig. 2G) and numerous Schwann cell cytoplasmic processes extended into the epidermis, reaching the stratum corneum by 42 days post-axotomy (Fig. 2F, Fig. 3B2 and B3). Schwann cell nuclei were located in the dermis and not identified within the epidermis. By 72 days post-axotomy, intra-epidermal Schwann cell processes had retracted with few remaining within epidermis. However, nerve bundles containing Schwann cells remained at the dermal-epidermal junction (Fig. 2H). Both during collateral and vertical regenerative phases, p75 was expressed at the growing terminals of the axons ensheathed by Schwann cells (Fig. 3A, Fig. 3 B2 and B3). Within the epidermis, p75 was densely expressed on the Schwann cells co-localized on unmyelinated axons stained with PGP 9.5 (Fig. 3 B1, B2, B3).

Thus, in summary, the epidermis was ultimately reinnervated by regenerating axons that entered the epidermis first as collateral sprouts at the excision margin or as branches of axons extending from the collateral sprouts at the dermal-epidermal junction, and then as vertically-oriented regenerating fibers extending from the dermis into the epidermis. In both patterns of reinnervation, axons entering the epidermis were ensheathed by p75+ Schwann cell processes. The expression of s100, another Schwann cell marker, was seen on the

dermal Schwann cells and Langerhans cells within the epidermis but not on the epidermal Schwann cell processes (Fig. 4).

### Measurement of intra-epidermal nerve fibers

The collateral sprouting epidermal nerve fibers (termed sprouts = S) reflected reinnervation into the excisional site that had been denervated by excisional axotomy. In uninfected animals, the longest collateral sprouts were present at Day 14 post-axotomy with a mean axonal length of sprouts was 108.2 $\mu$ m (SD 43.4 $\mu$ m). In contrast, collateral sprout length at Day 70 post-axotomy was shorter at 45.5  $\mu$ m (SD 9.2 $\mu$ m). The mean length of collateral sprouts across all time points was 72.3  $\mu$ m (SD 22.7 $\mu$ m; Fig. 5). The epidermal nerve fibers lying outside the initial axotomy zone, (termed normal = N) were measured as they were representative of normal fiber length independent of axotomy. Mean normal fiber length was 46.6  $\mu$ m (SD 2.3 $\mu$ m).

### Effects of SIV infection on epidermal nerve fiber length post-axotomy

Similar to uninfected macaques, the longest collateral sprouts in SIV-infected animals were present at Day 14 post-axotomy but these sprouts had a shorter mean sprouting axonal length of 102.6  $\mu$ m (SD 24.02 $\mu$ m) versus control animals (108.2 $\mu$ m). Collateral sprout length at day 70 post-axotomy was shorter at 57.1  $\mu$ m (SD 13.32 $\mu$ m). The mean length of collateral sprouts across all time points was 81.2  $\mu$ m (SD 17.14 $\mu$ m) and outside the excision line at the edge of the sample the length of uninjured axons was 48.9  $\mu$ m (SD 4.3 $\mu$ m).

To compare epidermal fiber lengths of both collateral sprouts and normal nerve fibers in control versus SIV-infected macaques given the large variation in fiber length between individual animals, we calculated the ratio of collateral sprout length to normal fiber length (S:N ratio) for each uninfected and SIV-infected animal at all time points post-axotomy (Fig. 5). In uninfected animals, the mean S:N ratio at Day 14 post-axotomy was 2.3, while the SIV infected group had a Day 14 post-axotomy mean of 1.9, indicating that sprout length was shorter in SIV-infected animals in the early time points after axotomy.

At ensuing time points post-axotomy, the uninfected group's change in S:N ratio over time was significantly greater than the rate of change for the SIV-infected group ( $p = 0.015$ , repeated measures regression). Specifically, the group of uninfected macaques had a 0.27 unit decrease in S:N ratio every 2 weeks while the SIV-infected group's S:N ratio declined, on average, 0.14 units per 14 days (Fig. 5).

### Effects of SIV infection on intra-epidermal Schwann cell density post-axotomy

Given our observation that Schwann cells appear to play a critical role in cutaneous nerve regeneration in macaques following axotomy, we measured and compared the epidermal density of Schwann cell processes in uninfected and SIV-infected animals to determine whether SIV infection altered Schwann cell process migration (Fig. 2F). The group of SIV-infected macaques had lower mean intraepidermal Schwann cell density measurements than the group of uninfected animals at all time points examined post-axotomy, from 14 to 70 days post-transection, however, the difference between groups was not significant at any of these time points post-axotomy ( $p > 0.05$ , t-test ; Fig. 6). In both SIV-infected and uninfected control animals, Schwann cell density was highest immediately after axotomy; the subsequent rate of decline in Schwann cell density over time did not differ significantly between the two groups ( $p = 0.178$  ; repeat measures regression).

## DISCUSSION

This study describes the epidermal reinnervation pattern in control and SIV-infected macaques using an excisional axotomy injury model. The dermal plexuses were transected via an excisional punch and subsequent axonal regrowth and reinnervation of epidermis were examined to determine 1) the normal course of nerve fiber repair in macaques and 2) whether SIV infection altered the pattern and/or kinetics of epidermal nerve fiber repair.

### Altered epidermal nerve regeneration in SIV-infected macaques

By measuring and comparing the ratio of collateral sprout length to normal fiber length (designated as S:N ratio) for uninfected and SIV-infected animal at progressive 14-day intervals post-axotomy, we found that sprout length was shorter in SIV-infected animals than uninfected control macaques in the early time points after axotomy. Furthermore, at ensuing time points post-axotomy, the uninfected group's change in S:N ratio over time was significantly greater than the SIV-infected group ( $p = 0.015$ , repeated measures regression). Together, these differences in epidermal nerve regeneration between control and SIV-infected animals demonstrate that SIV-infection alters the kinetics of epidermal nerve fiber regeneration following axotomy. It will be important to confirm whether HIV causes a similar change in epidermal fiber regeneration in infected individuals since this finding would direct future therapeutic approaches.

As Schwann cell migration into the denervated epidermis may play a crucial role in guiding axonal regrowth, we also measured epidermal Schwann cell density in SIV-infected versus control animals to determine whether SIV infection altered Schwann cell migration patterns post-axotomy. In this study, we found a trend towards slower migration of Schwann cells into the denervated epidermis following axotomy in SIV-infected animal versus control macaques. At every time point evaluated post-axotomy, there were fewer epidermal Schwann cells in SIV-infected animals versus uninfected macaques, suggesting that Schwann cell guidance and support of epidermal nerve fiber regeneration may account for the altered nerve regeneration seen in SIV-infected animals. Given the heterogeneity within the SIV and uninfected groups, increasing the group size would aid in defining the role of Schwann cells during regeneration.

Together, these findings illustrate the value of the SIV/macaque model for investigating the mechanisms underlying HIV-induced alterations in cutaneous nerve regeneration. Neuronal loss due to macrophage infiltration occurs in somatosensory ganglia of SIV-infected macaques (Laast et al., 2007). In vitro modeling using rat dorsal root ganglia cultures has suggested that Schwann cells play an important role in mediating HIV-1 gp120 toxicity by producing the chemokine RANTES that causes both neuritic degeneration and TNF- $\alpha$ -mediated neuronal apoptosis (Keswani et al., 2003). Impaired reinnervation has also been observed in the distal leg of HIV-infected individuals, (Hahn et al., 2007). Additional studies in SIV-infected macaques may help to define the specific Schwann cell-axon interactions relevant to the pathogenesis of HIV-associated sensory neuropathies.

### Differences in axonal regeneration between juvenile macaques and human adults

In macaques, rapid and complete reinnervation of the epidermis occurred in both uninfected and SIV-infected macaques after intracutaneous axotomy. The relatively rapid rate of reinnervation in macaques contrasted with the slower rate reported in healthy humans. All examined monkeys had complete reinnervation of the epidermis by the 56th day after axotomy. In contrast, in healthy humans, we previously showed that reinnervation of epidermis was incomplete even 23 months after axotomy (Rajan et al., 2003). Although this difference may represent enhanced, or perhaps more efficient, regenerative regrowth in the

macaque, we examined juvenile macaques in this study whereas the human studies evaluated only adults over the age of 30 years. The rate of epidermal reinnervation following damage may therefore be an age-dependent process in primates. Alternately, there may be species-specific differences in the rates of regeneration after axotomy.

We also noted morphologic differences in the patterns of reinnervation post-axotomy between humans and macaques. In the human excision model, collateral nerve sprouts originated from the epidermal axons at the margin of the axotomy excision line but regenerating axons did not enter the epidermis through the underlying dermis. In contrast, in macaques, collateral sprouting of axons from the adjacent uninjured superficial dermal nerve bundles was the initial regenerative response following axotomy and contributed to the initial phase of reinnervation in the epidermis. The axons directly entered the epidermis, extending from p75+ Schwann cell-rich uninjured nerve bundles at the excision margin. The axonal elongation was particularly rapid during the first two weeks of the regeneration period. Axons also sprouted from the nerve bundles that migrated along the basement membrane and subsequently numerous branches entered vertically to produce the intra-epidermal axons. Later, dense vertical regeneration of axons growing through the dermis completed the epidermal reinnervation of the central excision zone. This pattern was not noted in humans, and suggests that regenerative regrowth may be more efficient in the juvenile macaques than mature humans. In fact, the regeneration patterns observed in the macaques are similar to regeneration in experimental rats where, after injury, both axonal regeneration and collateral sprouting contribute towards the reinnervation of the skin (Diamond et al., 1992; Jackson and Diamond, 1984; Jancso and Kiraly, 1983; Verdu and Navarro, 1997). Additional studies that address the influence of subject age on reinnervation are needed to clarify whether the observed differences are attributable to age-dependent or species-specific changes in post-axotomy regeneration patterns. Exploring the barriers to regenerative regrowth in humans might have obvious therapeutic relevance.

### **Schwann cell migration in macaques**

Within the epidermis at the excision site, there was rapid inwards migration of p75 positive Schwann cell processes leading to increased Schwann cell density in comparison to normal skin. Enhanced expression of p75 on the persisting Schwann cell bands, the growing edge of the axonal sprouts, and the realignment of the Schwann cell bands towards the epidermis were noted. In contrast, in a human excision model, the Schwann cells at the denervated zone of the dermis remained flattened and did not re-orient towards the epidermis until fully 23 months after axotomy (Rajan et al., 2003). Other studies also have shown that p75+ nerve fibers are infrequent in normal epidermis (Liang and Johansson, 1998; Liang et al., 1999; Taniguchi et al., 2007).

A number of studies have indicated that Schwann cells play a vital role in the regeneration of axons after injury (Albers and Davis, 2007a; Anton et al., 1994; Bentley and Lee, 2000; Griffin et al., 1996; Griffin et al., 2006; Song et al., 2006; Taniguchi et al., 2007; Terenghi, 1999). In humans as well as in rodents, experimental studies suggest that nerves adjacent to atrophic Schwann cells have impaired nerve regeneration and compromised myelin production (Ebenezer et al., 2007b; Fu and Gordon, 1995; 1997; Furey et al., 2007; Heine et al., 2004; Hoke et al., 2002; Midha et al., 2005; Ohnishi and Dyck, 1981; Sulaiman et al., 2002; Tomita et al., 2007). Studies also have shown that Schwann cells produce extracellular matrix (ECM) components that may be organized to form basal lamina. Schwann cells can interact with different basement membrane components including laminin isoforms, collagen IV, and fibronectin (Chen et al., 2005; Chernousov et al., 2001; Donzelli et al., 2006; McKee et al., 2007) and also have been shown to be rich sources of nerve growth factor (NGF) (Ard et al., 1987; Bunge et al., 1987; Bunge et al., 1986; Carey et al., 1983; Cornbrooks et al., 1983). Neurotrophins are essential for axonal guidance,

migration, and elongation in the peripheral nervous system (Ahmed et al., 1999; Bentley and Lee, 2000; Boyd and Gordon, 2003; Diamond et al., 1992; Fields et al., 1989; Hall, 2005; Hoke, 2006; Liang and Johansson, 1998).

Neurotrophic growth factors support diverse population of sensory axons. Unmyelinated C and small, thinly myelinated A $\delta$  fiber types are supported by NGF (Albers and Davis, 2007b; Lopez et al., 1998; Murinson et al., 2005b; Rice et al., 1998). In the present study, the finding of Schwann cell process extension into the epidermis with high expression of p75 at 14 days post-axotomy may provide a permissive environment favorable for axonal regrowth in the epidermis. (Bentley and Lee, 2000; Griffin and Thompson, 2008; Johnson, 1988; Murinson et al., 2005a; Taniuchi et al., 1988; Tomita et al., 2007; Yamashita et al., 1999; You et al., 1997).

In vitro studies indicate that proliferating keratinocytes are a major source of NGF, thus it is possible that keratinocyte production of NGF may decrease post-proliferation (i.e with keratinocyte maturation) thereby providing less support for intra-epidermal Schwann cells (Albers and Davis, 2007a; Marconi et al., 2003; Pincelli and Marconi, 2000; Pincelli et al., 1994). The Schwann cell ensheathment at the leading edge of the regenerating axons supports the finding that the Schwann cells are guiding the pathway for the axons to reach the target (Bunge et al., 1987; Guenard et al., 1992; Thompson and Buettner, 2006).

In contrast to nerve repair in the human excision model, extracellular matrix and epidermal keratinocytes may provide a more favorable environment for promoting Schwann cell and axonal re-growth in macaques. Schwann cells may respond to the basement membrane as a supportive substrate that encourages their migration to the mid-axotomy zone. Species-specific differences in the ECM or components of the dermal-epidermal junction may account for the variability in the migration patterns of Schwann cell processes into epidermis between macaques and man. In mice, it has been demonstrated that in a normal neuromuscular junction, Schwann cells can ensheath motor axons, except at the post-synaptic basement membrane. Laminin 11, a heterotrimeric glycoprotein (Yang et al., 2005) neuromuscular junction (Cho et al., 1998; Patton et al., 1998). In contrast, in primates, laminin 2 has shown neurite-promoting and cell attachment activities (Wallquist et al., 2005; Yang et al., 2005). In addition, a unique epithelial basement membrane antigen KF-1 demonstrates specific binding to the lamina densa of the basement membrane of stratified squamous epithelia (Breathnach et al., 1983; Fine et al., 1987). More studies are needed to establish the relationship between Schwann cell interaction with ECM and other components at the dermal epidermal junction in both human and animal skin. Decreased s100 immunoreactivity along epidermal Schwann cells is consistent with heterogeneity within nonmyelinating Schwann cell populations and suggests that Schwann cells may be supporting regeneration in a phenotype-specific manner with respect to levels of both p75 and s100 (Bentley and Lee, 2000; Hoke et al., 2006; Scherer et al., 1994; You et al., 1997).

In conclusion, this study identified that SIV infection alters epidermal nerve repair including both the kinetics of axonal regrowth and Schwann cell migration into epidermis. A difference in the pattern of epidermal reinnervation of macaques after intracutaneous axotomy compared to humans was also identified. Our animal excision model suggests that nerve regeneration patterns may be related to the species-specific patterns of migration of Schwann cells. However, the impact of age on these repair processes remains to be established. In addition, these studies were performed on skin from the back and additional study will be needed to determine whether cutaneous reinnervation differs in skin of the hands and feet where clinical manifestations of sensory neuropathies are most evident. The shorter time required for regeneration and the accelerated nerve regeneration time-course in

juvenile macaques provides a useful model for studying neurotrophic and regenerative drugs for translational research and human clinical trials of neuropathies.

## Acknowledgments

The authors thank Ryan O'Donnell, Jennifer Killen, Jamie Dorsey and Suzanne Queen for expert technical assistance.

This study was supported by National Institutes of Health grants to JCM (NS44807, NS 049465, and P30MH075673) and NS055651 (JLM). This work also was supported by U54NS043011 (to E Kraiselburd; JHU site PI JCM) and P01MH070056 (A Nath: Project PIs JCM and MCZ).

## REFERENCES

- Ahmed Z, Brown RA, Ljungberg C, Wiberg M, Terenghi G. Nerve growth factor enhances peripheral nerve regeneration in non-human primates. *Scand J Plast Reconstr Surg Hand Surg.* 1999; 33:393–401. [PubMed: 10614747]
- Albers KM, Davis BM. The skin as a neurotrophic organ. *Neuroscientist.* 2007a; 13:371–382. [PubMed: 17644767]
- Anton ES, Weskamp G, Reichardt LF, Matthew WD. Nerve growth factor and its low-affinity receptor promote Schwann cell migration. *Proc Natl Acad Sci U S A.* 1994; 91:2795–2799. [PubMed: 8146193]
- Ard MD, Bunge RP, Bunge MB. Comparison of the Schwann cell surface and Schwann cell extracellular matrix as promoters of neurite growth. *J Neurocytol.* 1987; 16:539–555. [PubMed: 3681353]
- Baudier J, Gerard D. Ions binding to S100 proteins. II. Conformational studies and calcium-induced conformational changes in S100 alpha alpha protein: the effect of acidic pH and calcium incubation on subunit exchange in S100a (alpha beta) protein. *J Biol Chem.* 1986; 261:8204–8212. [PubMed: 3722150]
- Bentley CA, Lee KF. p75 is important for axon growth and schwann cell migration during development. *J Neurosci.* 2000; 20:7706–7715. [PubMed: 11027232]
- Boyd JG, Gordon T. Neurotrophic factors and their receptors in axonal regeneration and functional recovery after peripheral nerve injury. *Mol Neurobiol.* 2003; 27:277–324. [PubMed: 12845152]
- Breathnach SM, Fox PA, Neises GR, Stanley JR, Katz SI. A unique epithelial basement membrane antigen defined by a monoclonal antibody (KF-1). *J Invest Dermatol.* 1983; 80:392–395. [PubMed: 6341473]
- Bunge MB, Johnson MI, Ard MD, Kleitman N. Factors influencing the growth of regenerating nerve fibers in culture. *Prog Brain Res.* 1987; 71:61–74. [PubMed: 3588964]
- Bunge RP, Bunge MB, Eldridge CF. Linkage between axonal ensheathment and basal lamina production by Schwann cells. *Annu Rev Neurosci.* 1986; 9:305–328. [PubMed: 3518587]
- Carey DJ, Eldridge CF, Cornbrooks CJ, Timpl R, Bunge RP. Biosynthesis of type IV collagen by cultured rat Schwann cells. *J Cell Biol.* 1983; 97:473–479. [PubMed: 6885907]
- Chen YY, McDonald D, Cheng C, Magnowski B, Durand J, Zochodne DW. Axon and Schwann cell partnership during nerve regrowth. *J Neuropathol Exp Neurol.* 2005; 64:613–622. [PubMed: 16042313]
- Chernousov MA, Stahl RC, Carey DJ. Schwann cell type V collagen inhibits axonal outgrowth and promotes Schwann cell migration via distinct adhesive activities of the collagen and noncollagen domains. *J Neurosci.* 2001; 21:6125–6135. [PubMed: 11487636]
- Cho SI, Ko J, Patton BL, Sanes JR, Chiu AY. Motor neurons and Schwann cells distinguish between synaptic and extrasynaptic isoforms of laminin. *J Neurobiol.* 1998; 37:339–358. [PubMed: 9828041]
- Clements JE, Babas T, Mankowski JL, Suryanarayana K, Piatak M Jr, Tarwater PM, Lifson JD, Zink MC. The central nervous system as a reservoir for simian immunodeficiency virus (SIV): steady-state levels of SIV DNA in brain from acute through asymptomatic infection. *J Infect Dis.* 2002; 186:905–913. [PubMed: 12232830]

- Cornblath DR, McArthur JC. Predominantly sensory neuropathy in patients with AIDS and AIDS-related complex. *Neurology*. 1988; 38:794–796. [PubMed: 2834669]
- Cornbrooks CJ, Carey DJ, McDonald JA, Timpl R, Bunge RP. In vivo and in vitro observations on laminin production by Schwann cells. *Proc Natl Acad Sci U S A*. 1983; 80:3850–3854. [PubMed: 6344090]
- Diamond J, Holmes M, Coughlin M. Endogenous NGF and nerve impulses regulate the collateral sprouting of sensory axons in the skin of the adult rat. *J Neurosci*. 1992; 12:1454–1466. [PubMed: 1556603]
- Donato R. S100: a multigenic family of calcium-modulated proteins of the EF-hand type with intracellular and extracellular functional roles. *Int J Biochem Cell Biol*. 2001; 33:637–668. [PubMed: 11390274]
- Donzelli R, Maiuri F, Piscopo GA, de Notaris M, Colella A, Divitiis E. Role of extracellular matrix components in facial nerve regeneration: an experimental study. *Neurol Res*. 2006; 28:794–801. [PubMed: 17288733]
- Dyck PJ, Kratz KM, Karnes JL, Litchy WJ, Klein R, Pach JM, Wilson DM, O'Brien PC, Melton LJ 3rd, Service FJ. The prevalence by staged severity of various types of diabetic neuropathy, retinopathy, and nephropathy in a population-based cohort: the Rochester Diabetic Neuropathy Study. *Neurology*. 1993; 43:817–824. [PubMed: 8469345]
- Ebenezer GJ, Hauer P, Gibbons C, McArthur JC, Polydefkis M. Assessment of epidermal nerve fibers: a new diagnostic and predictive tool for peripheral neuropathies. *J Neuropathol Exp Neurol*. 2007a; 66:1059–1073. [PubMed: 18090915]
- Ebenezer GJ, McArthur JC, Thomas D, Murinson B, Hauer P, Polydefkis M, Griffin JW. Denervation of skin in neuropathies: the sequence of axonal and Schwann cell changes in skin biopsies. *Brain*. 2007b; 130:2703–2714. [PubMed: 17898011]
- Fields RD, Le Beau JM, Longo FM, Ellisman MH. Nerve regeneration through artificial tubular implants. *Prog Neurobiol*. 1989; 33:87–134. [PubMed: 2678271]
- Fine JD, Redmar DA, Goodman AL. Sequence of reconstitution of seven basement-membrane components following split-thickness wound induction in primate skin. *Arch Dermatol*. 1987; 123:1174–1178. [PubMed: 3632002]
- Fu SY, Gordon T. Contributing factors to poor functional recovery after delayed nerve repair: prolonged axotomy. *J Neurosci*. 1995; 15:3876–3885. [PubMed: 7751952]
- Fu SY, Gordon T. The cellular and molecular basis of peripheral nerve regeneration. *Mol Neurobiol*. 1997; 14:67–116. [PubMed: 9170101]
- Furey MJ, Midha R, Xu QG, Belkas J, Gordon T. Prolonged target deprivation reduces the capacity of injured motoneurons to regenerate. *Neurosurgery*. 2007; 60:723–732. discussion 732-723. [PubMed: 17415210]
- Gibbons CH, Griffin JW, Polydefkis M, Bonyhay I, Brown A, Hauer PE, McArthur JC. The utility of skin biopsy for prediction of progression in suspected small fiber neuropathy. *Neurology*. 2006; 66:256–258. [PubMed: 16434668]
- Griffin JW, George EB, Chaudhry V. Wallerian degeneration in peripheral nerve disease. *Baillieres Clin Neurol*. 1996; 5:65–75. [PubMed: 8732200]
- Griffin JW, Hoke A, Nguyen TT. Textbook of neural repair and rehabilitation. In: Michael E, Selzer; Stephanie, Clarke; Leonardo, Cohen; Pamela, Duncan; Fred, Gage, editors. *Neural repair and plasticity*. Chapter 17. Vol. 1. Cambridge: Cambridge University Press; 2006. p. 293-303.
- Griffin JW, Thompson WJ. Biology and pathology of nonmyelinating Schwann cells. *Glia*. 2008; 56:1518–1531. [PubMed: 18803315]
- Guenard V, Kleitman N, Morrissey TK, Bunge RP, Aebischer P. Syngeneic Schwann cells derived from adult nerves seeded in semipermeable guidance channels enhance peripheral nerve regeneration. *J Neurosci*. 1992; 12:3310–3320. [PubMed: 1527582]
- Hahn K, Triolo A, Hauer P, McArthur JC, Polydefkis M. Impaired reinnervation in HIV infection following experimental denervation. *Neurology*. 2007; 68:1251–1256. [PubMed: 17438214]
- Haigwood NL. Predictive value of primate models for AIDS. *AIDS Rev*. 2004; 6:187–198. [PubMed: 15700617]

- Hall S. The response to injury in the peripheral nervous system. *J Bone Joint Surg Br.* 2005; 87:1309–1319. [PubMed: 16189300]
- Heine W, Conant K, Griffin JW, Hoke A. Transplanted neural stem cells promote axonal regeneration through chronically denervated peripheral nerves. *Exp Neurol.* 2004; 189:231–240. [PubMed: 15380475]
- Herrmann DN, McDermott MP, Henderson D, Chen L, Akowuah K, Schifitto G. Epidermal nerve fiber density, axonal swellings and QST as predictors of HIV distal sensory neuropathy. *Muscle Nerve.* 2004; 29:420–427. [PubMed: 14981742]
- Herrmann DN, McDermott MP, Sowden JE, Henderson D, Messing S, Cruttenden K, Schifitto G. Is skin biopsy a predictor of transition to symptomatic HIV neuropathy? A longitudinal study. *Neurology.* 2006; 66:857–861. [PubMed: 16567702]
- Hirai A, Yasuda H, Joko M, Maeda T, Kikkawa R. Evaluation of diabetic neuropathy through the quantitation of cutaneous nerves. *J Neurol Sci.* 2000; 172:55–62. [PubMed: 10620661]
- Hoke A. Mechanisms of Disease: what factors limit the success of peripheral nerve regeneration in humans? *Nat Clin Pract Neurol.* 2006; 2:448–454. [PubMed: 16932603]
- Hoke A, Gordon T, Zochodne DW, Sulaiman OA. A decline in glial cell-line-derived neurotrophic factor expression is associated with impaired regeneration after long-term Schwann cell denervation. *Exp Neurol.* 2002; 173:77–85. [PubMed: 11771940]
- Hoke A, Redett R, Hameed H, Jari R, Zhou C, Li ZB, Griffin JW, Brushart TM. Schwann cells express motor and sensory phenotypes that regulate axon regeneration. *J Neurosci.* 2006; 26:9646–9655. [PubMed: 16988035]
- Jackson PC, Diamond J. Temporal and spatial constraints on the collateral sprouting of low-threshold mechanosensory nerves in the skin of rats. *J Comp Neurol.* 1984; 226:336–345. [PubMed: 6747026]
- Jancso G, Kiraly E. Cutaneous nerve regeneration in the rat: reinnervation of the denervated skin by regenerative but not by collateral sprouting. *Neurosci Lett.* 1983; 36:133–137. [PubMed: 6306517]
- Johnson EM Jr. Regulation of nerve growth factor receptor expression on Schwann cells. *Prog Brain Res.* 1988; 78:327–331. [PubMed: 2854638]
- Kar BR, Job CK. Visible deformity in childhood leprosy--a 10-year study. *Int J Lepr Other Mycobact Dis.* 2005; 73:243–248. [PubMed: 16830633]
- Kennedy, WR.; Wendelschafer-Crabb, G.; Polydefkis, M.; McArthur, JC. Pathology and quantitation of cutaneous innervation. In: Dyck, PJ.; Thomas, PK., editors. *Peripheral Neuropathy.* 4th edn.. Philadelphia: Saunders; 2005. p. 869-896.
- Kennedy WR, Wendelschafer-Crabb G. The innervation of human epidermis. *J Neurol Sci.* 1993; 115:184–190. [PubMed: 8482979]
- Keswani SC, Polley M, Pardo CA, Griffin JW, McArthur JC, Hoke A. Schwann cell chemokine receptors mediate HIV-1 gp120 toxicity to sensory neurons. *Ann Neurol.* 2003; 54:287–296. [PubMed: 12953261]
- Laast VA, Pardo CA, Tarwater PM, Queen SE, Reinhart TA, Ghosh M, Adams RJ, Zink MC, Mankowski JL. Pathogenesis of simian immunodeficiency virus-induced alterations in macaque trigeminal ganglia. *J Neuropathol Exp Neurol.* 2007; 66:26–34. [PubMed: 17204934]
- Lauria G, Cornblath DR, Johansson O, McArthur JC, Mellgren SI, Nolano M, Rosenberg N, Sommer C. EFNS guidelines on the use of skin biopsy in the diagnosis of peripheral neuropathy. *Eur J Neurol.* 2005; 12:747–758. [PubMed: 16190912]
- Lauria G, Morbin M, Lombardi R, Borgna M, Mazzoleni G, Sghirlanzoni A, Pareyson D. Axonal swellings predict the degeneration of epidermal nerve fibers in painful neuropathies. *Neurology.* 2003; 61:631–636. [PubMed: 12963753]
- Liang Y, Johansson O. Light and electron microscopic demonstration of the p75 nerve growth factor receptor in normal human cutaneous nerve fibers: new vistas. *J Invest Dermatol.* 1998; 111:114–118. [PubMed: 9665396]
- Liang Y, Marcusson JA, Johansson O. Light and electron microscopic immunohistochemical observations of p75 nerve growth factor receptor-immunoreactive dermal nerves in prurigo nodularis. *Arch Dermatol Res.* 1999; 291:14–21. [PubMed: 10025723]

- Lichtenstein KA, Armon C, Baron A, Moorman AC, Wood KC, Holmberg SD. Modification of the incidence of drug-associated symmetrical peripheral neuropathy by host and disease factors in the HIV outpatient study cohort. *Clin Infect Dis*. 2005; 40:148–157. [PubMed: 15614705]
- Lopez SM, Perez-Perez M, Marquez JM, Naves FJ, Represa J, Vega JA. p75 and TrkA neurotrophin receptors in human skin after spinal cord and peripheral nerve injury, with special reference to sensory corpuscles. *Anat Rec*. 1998; 251:371–383. [PubMed: 9669765]
- Mankowski JL, Clements JE, Zink MC. Searching for clues: tracking the pathogenesis of human immunodeficiency virus central nervous system disease by use of an accelerated, consistent simian immunodeficiency virus macaque model. *J Infect Dis*. 2002a; 186 Suppl 2:S199–S208. [PubMed: 12424698]
- Mankowski JL, Queen SE, Clements JE, Zink MC. Cerebrospinal fluid markers that predict SIV CNS disease. *J Neuroimmunol*. 2004; 157:66–70. [PubMed: 15579282]
- Mankowski JL, Queen SE, Tarwater PM, Fox KJ, Perry VH. Accumulation of beta-amyloid precursor protein in axons correlates with CNS expression of SIV gp41. *J Neuropathol Exp Neurol*. 2002b; 61:85–90. [PubMed: 11829347]
- Marconi A, Terracina M, Fila C, Franchi J, Bonte F, Romagnoli G, Maurelli R, Failla CM, Dumas M, Pincelli C. Expression and function of neurotrophins and their receptors in cultured human keratinocytes. *J Invest Dermatol*. 2003; 121:1515–1521. [PubMed: 14675204]
- McArthur JC, Brew BJ, Nath A. Neurological complications of HIV infection. *Lancet Neurol*. 2005; 4:543–555. [PubMed: 16109361]
- McArthur JC, Griffin JW. Another tool for the neurologist's toolbox. *Ann Neurol*. 2005; 57:163–167. [PubMed: 15668978]
- McArthur JC, Stocks EA, Hauer P, Cornblath DR, Griffin JW. Epidermal nerve fiber density: normative reference range and diagnostic efficiency. *Arch Neurol*. 1998; 55:1513–1520. [PubMed: 9865794]
- McCarthy BG, Hsieh ST, Stocks A, Hauer P, Macko C, Cornblath DR, Griffin JW, McArthur JC. Cutaneous innervation in sensory neuropathies: evaluation by skin biopsy. *Neurology*. 1995; 45:1848–1855. [PubMed: 7477980]
- McKee KK, Harrison D, Capizzi S, Yurchenco PD. Role of laminin terminal globular domains in basement membrane assembly. *J Biol Chem*. 2007; 282:21437–21447. [PubMed: 17517882]
- Midha R, Munro CA, Chan S, Nitising A, Xu QG, Gordon T. Regeneration into protected and chronically denervated peripheral nerve stumps. *Neurosurgery*. 2005; 57:1289–1299. [PubMed: 16331178]
- Murinson BB, Archer DR, Li Y, Griffin JW. Degeneration of myelinated efferent fibers prompts mitosis in Remak Schwann cells of uninjured C-fiber afferents. *J Neurosci*. 2005a; 25:1179–1187. [PubMed: 15689554]
- Murinson BB, Hoffman PN, Banihashemi MR, Meyer RA, Griffin JW. C-fiber (Remak) bundles contain both isolectin B4-binding and calcitonin gene-related peptide-positive axons. *J Comp Neurol*. 2005b; 484:392–402. [PubMed: 15770655]
- Ohnishi A, Dyck PJ. Retardation of Schwann cell division and axonal regrowth following nerve crush in experimental lead neuropathy. *Ann Neurol*. 1981; 10:469–477. [PubMed: 7305299]
- Ownby KK, Dune LS. The processes by which persons with HIV-related peripheral neuropathy manage their symptoms: a qualitative study. *J Pain Symptom Manage*. 2007; 34:48–59. [PubMed: 17532177]
- Patton BL, Chiu AY, Sanes JR. Synaptic laminin prevents glial entry into the synaptic cleft. *Nature*. 1998; 393:698–701. [PubMed: 9641682]
- Pincelli C, Marconi A. Autocrine nerve growth factor in human keratinocytes. *J Dermatol Sci*. 2000; 22:71–79. [PubMed: 10674819]
- Pincelli C, Sevignani C, Manfredini R, Grande A, Fantini F, Bracci-Laudiero L, Aloe L, Ferrari S, Cossarizza A, Giannetti A. Expression and function of nerve growth factor and nerve growth factor receptor on cultured keratinocytes. *J Invest Dermatol*. 1994; 103:13–18. [PubMed: 8027574]

- Polydefkis M, Hauer P, Sheth S, Sirdofsky M, Griffin JW, McArthur JC. The time course of epidermal nerve fibre regeneration: studies in normal controls and in people with diabetes, with and without neuropathy. *Brain*. 2004; 127:1606–1615. [PubMed: 15128618]
- Polydefkis M, Sirdofsky M, Hauer P, Petty BG, Murinson B, McArthur JC. Factors influencing nerve regeneration in a trial of timcodar dimesylate. *Neurology*. 2006; 66:259–261. [PubMed: 16434669]
- Polydefkis M, Yiannoutsos CT, Cohen BA, Hollander H, Schifitto G, Clifford DB, Simpson DM, Katzenstein D, Shriver S, Hauer P, Brown A, Haidich AB, Moo L, McArthur JC. Reduced intraepidermal nerve fiber density in HIV-associated sensory neuropathy. *Neurology*. 2002; 58:115–119. [PubMed: 11781415]
- Rajan B, Polydefkis M, Hauer P, Griffin JW, McArthur JC. Epidermal reinnervation after intracutaneous axotomy in man. *J Comp Neurol*. 2003; 457:24–36. [PubMed: 12541322]
- Rice FL, Albers KM, Davis BM, Silos-Santiago I, Wilkinson GA, LeMaster AM, Ernfors P, Smeyne RJ, Aldskogius H, Phillips HS, Barbacid M, DeChiara TM, Yancopoulos GD, Dunne CE, Fundin BT. Differential Dependency of Unmyelinated and A[delta] Epidermal and Upper Dermal Innervation on Neurotrophins, Trk Receptors, and p75LNGFR. *Developmental Biology*. 1998; 198:57–81. [PubMed: 9640332]
- Rice FL, Rasmusson DD. Innervation of the digit on the forepaw of the raccoon. *J Comp Neurol*. 2000; 417:467–490. [PubMed: 10701867]
- Ross AH, Grob P, Bothwell M, Elder DE, Ernst CS, Marano N, Ghrist BF, Slemp CC, Herlyn M, Atkinson B, et al. Characterization of nerve growth factor receptor in neural crest tumors using monoclonal antibodies. *Proc Natl Acad Sci U S A*. 1984; 81:6681–6685. [PubMed: 6093111]
- Scherer SS, Xu YT, Roling D, Wrabetz L, Feltri ML, Kamholz J. Expression of growth-associated protein-43 kD in Schwann cells is regulated by axon-Schwann cell interactions and cAMP. *J Neurosci Res*. 1994; 38:575–589. [PubMed: 7815473]
- So YT, Holtzman DM, Abrams DI, Olney RK. Peripheral neuropathy associated with acquired immunodeficiency syndrome. Prevalence and clinical features from a population-based survey. *Arch Neurol*. 1988; 45:945–948. [PubMed: 2843154]
- Song XY, Zhou FH, Zhong JH, Wu LL, Zhou XF. Knockout of p75(NTR) impairs re-myelination of injured sciatic nerve in mice. *J Neurochem*. 2006; 96:833–842. [PubMed: 16336221]
- Stocks EA, McArthur JC, Griffen JW, Mouton PR. An unbiased method for estimation of total epidermal nerve fibre length. *J Neurocytol*. 1996; 25:637–644. [PubMed: 9013425]
- Sulaiman OA, Midha R, Munro CA, Matsuyama T, Al-Majed A, Gordon T. Chronic Schwann cell denervation and the presence of a sensory nerve reduce motor axonal regeneration. *Exp Neurol*. 2002; 176:342–354. [PubMed: 12359176]
- Taniguchi M, Matsuzaki S, Tohyama M. P75 plays a key role in the induction of the sprouting of sensory nerve fibers in inflamed skin. *J Invest Dermatol*. 2007; 127:2062–2065. [PubMed: 17410199]
- Taniuchi M, Clark HB, Schweitzer JB, Johnson EM Jr. Expression of nerve growth factor receptors by Schwann cells of axotomized peripheral nerves: ultrastructural location, suppression by axonal contact, and binding properties. *J Neurosci*. 1988; 8:664–681. [PubMed: 2828568]
- Terenghi G. Peripheral nerve regeneration and neurotrophic factors. *J Anat*. 1999; 194(Pt 1):1–14. [PubMed: 10227662]
- Thompson DM, Buettner HM. Neurite outgrowth is directed by schwann cell alignment in the absence of other guidance cues. *Ann Biomed Eng*. 2006; 34:161–168. [PubMed: 16453203]
- Tomita K, Kubo T, Matsuda K, Fujiwara T, Yano K, Winograd JM, Tohyama M, Hosokawa K. The neurotrophin receptor p75NTR in Schwann cells is implicated in remyelination and motor recovery after peripheral nerve injury. *Glia*. 2007; 55:1199–1208. [PubMed: 17600367]
- Van Rompay KK, Singh RP, Heneine W, Johnson JA, Montefiori DC, Bischofberger N, Marthas ML. Structured treatment interruptions with tenofovir monotherapy for simian immunodeficiency virus-infected newborn macaques. *J Virol*. 2006; 80:6399–6410. [PubMed: 16775328]
- Verdu E, Navarro X. Comparison of immunohistochemical and functional reinnervation of skin and muscle after peripheral nerve injury. *Exp Neurol*. 1997; 146:187–198. [PubMed: 9225752]

- Wallquist W, Plantman S, Thams S, Thyboll J, Kortessmaa J, Lannergren J, Domogatskaya A, Ogren SO, Risling M, Hammarberg H, Tryggvason K, Cullheim S. Impeded interaction between Schwann cells and axons in the absence of laminin alpha4. *J Neurosci.* 2005; 25:3692–3700. [PubMed: 15814800]
- Wendelschafer-Crabb G, Kennedy WR, Walk D. Morphological features of nerves in skin biopsies. *J Neurol Sci.* 2006; 242:15–21. [PubMed: 16448669]
- Wilkinson KD, Lee KM, Deshpande S, Duerksen-Hughes P, Boss JM, Pohl J. The neuron-specific protein PGP 9.5 is a ubiquitin carboxyl-terminal hydrolase. *Science.* 1989; 246:670–673. [PubMed: 2530630]
- Yamashita T, Tucker KL, Barde YA. Neurotrophin binding to the p75 receptor modulates Rho activity and axonal outgrowth. *Neuron.* 1999; 24:585–593. [PubMed: 10595511]
- Yang D, Bierman J, Tarumi YS, Zhong YP, Rangwala R, Proctor TM, Miyagoe-Suzuki Y, Takeda S, Miner JH, Sherman LS, Gold BG, Patton BL. Coordinate control of axon defasciculation and myelination by laminin-2 and -8. *J Cell Biol.* 2005; 168:655–666. [PubMed: 15699217]
- You S, Petrov T, Chung PH, Gordon T. The expression of the low affinity nerve growth factor receptor in long-term denervated Schwann cells. *Glia.* 1997; 20:87–100. [PubMed: 9179594]
- Zhou L, Kitch DW, Evans SR, Hauer P, Raman S, Ebenezer GJ, Gerschenson M, Marra CM, Valcour V, Diaz-Arrastia R, Goodkin K, Millar L, Shriver S, Asmuth DM, Clifford DB, Simpson DM, McArthur JC. Correlates of epidermal nerve fiber densities in HIV-associated distal sensory polyneuropathy. *Neurology.* 2007; 68:2113–2119. [PubMed: 17562831]
- Ziegler D, Gries FA, Spuler M, Lessmann F. The epidemiology of diabetic neuropathy. Diabetic Cardiovascular Autonomic Neuropathy Multicenter Study Group. *J Diabetes Complications.* 1992; 6:49–57. [PubMed: 1562759]
- Zink MC, Coleman GD, Mankowski JL, Adams RJ, Tarwater PM, Fox K, Clements JE. Increased macrophage chemoattractant protein-1 in cerebrospinal fluid precedes and predicts simian immunodeficiency virus encephalitis. *J Infect Dis.* 2001; 184:1015–1021. [PubMed: 11574916]
- Zink MC, Laast VA, Helke KL, Brice AK, Barber SA, Clements JE, Mankowski JL. From mice to macaques--animal models of HIV nervous system disease. *Curr HIV Res.* 2006; 4:293–305. [PubMed: 16842082]

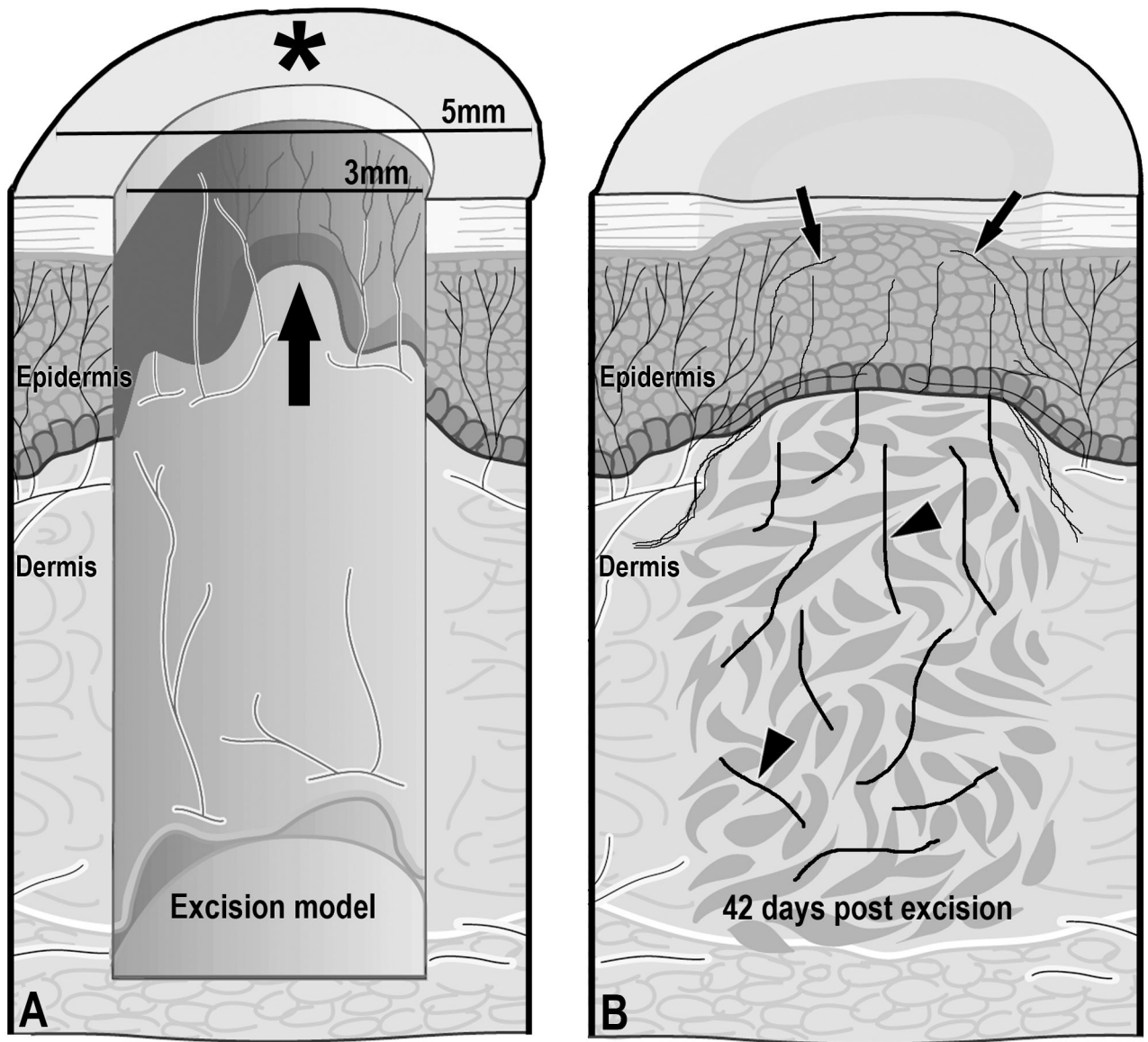


**Figure 1. An Intracutaneous Excisional Axotomy Model in Macaques**

Circular cutaneous axotomies were performed at 2-week intervals on the dorsal interscapular skin using a three mm skin punch to transect epidermal axons (Fig. 1A). The central core containing epidermis and dermis was then removed (arrow) yielding an excisional axotomy. On the 70th day after the initial axotomy, a five mm circular biopsy punch (\*) was used to harvest all of the previous three mm punch sites, providing samples containing axotomy sites that were 14, 28, 42, 56 and 70 days post-axotomy (Fig. 1A). By 42 days post-axotomy, collateral sprouts (arrows) and regenerating axons (arrowheads) had re-innervated the epidermis (Fig. 1B)

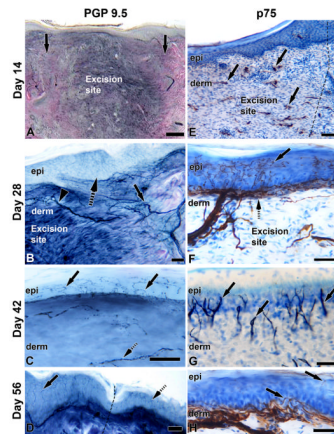


**Figure 2.**  
**A–D: Axonal regeneration in post- axotomy sections immunostained for the axonal marker PGP 9.5.**

At day 14 post-axotomy, the central denervated zone in both epidermis and dermis was devoid of axons. Arrows indicate excisional margin (A). By 28 days post-axotomy, along the excisional margin, intense immunoreactivity for PGP 9.5 was seen on the uninjured nerve bundles (arrow). Axons sprouted (hatched arrow) from these uninjured bundles and directly entered the denervated epidermis. Note that the supra-basal axons were elongated and leaned (hatched arrow) towards the denervated zone. Axons also formed thin nerve bundles (arrowhead) that extended horizontally along the dermal-epidermal junction toward the central denervated zone (B). Regenerating axons (hatched arrow) grew through the dermal collagen and entered the epidermis with a vertical orientation (arrows) that completed the epidermal reinnervation by Day 42 to 56 (C). Within the epidermis, the leaning collateral sprouts along the excision margin (dotted line) then retracted and straightened (arrow) resulting in epidermal nerve fibers within denervated sites that matched the orientation of uninjured axons in normal epidermis outside the excision site (hatched arrow; D). Scale bars= 200  $\mu\text{m}$  in A, 50  $\mu\text{m}$  in B–D.

**E–H: Schwann cells in post- axotomy sections immunostained for p75.**

At Day 14, in the center of the excision site p75 + Schwann cell bands (arrows) were oriented horizontally to the epidermal surface. The dotted line indicates excisional margin (E). From the excisional margin, the Schwann cells with collateral sprouts extended horizontally towards the middle of the excision site along the dermal-epidermal junction (hatched arrow). Schwann cell cytoplasmic processes (arrows) entered the denervated epidermis by 28 days and extended to the stratum corneum (the outermost keratinized epidermal layer; F). By 42 days, Schwann cell bands in the central denervated zone of the dermis were re-oriented perpendicular to the epidermal surface, parallel to each other (arrows) and also migrated from the papillary dermis into the epidermis (G, DAB stained section highlighted with nickel solution). In contrast, rare p75 + Schwann cell processes (arrows) remained within the epidermis at Day 56 (H). Scale bars= 100  $\mu\text{m}$  in E, 50  $\mu\text{m}$  in F–H.

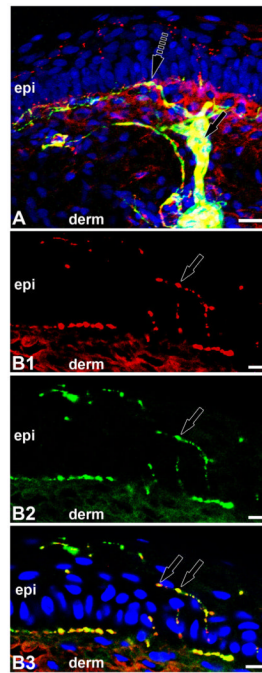


**Figure 3. Confocal microscopy montage of a 50µm section 28 days post axotomy, triple stained with the Schwann cell marker p75 (green), the axonal marker PGP9.5 (red) and the nuclear marker DraQ 5 (blue) to examine the relationship between axons and p75 expression** In the dermis, p75 was densely expressed at the excision line (arrow), in close association with PGP9.5 immunopositive nerve fibers in uninjured nerve bundles. Axons also sprouted and formed thin nerve bundles (hatched arrow, red) that extended along the dermal-epidermal junction adjacent to the basement membrane (A). Axons (red) branched from these bundles and entered the epidermis (arrow; B1). In the epidermis, p75 positive Schwann cell processes (green: B2) co-localized (yellow; arrow, B3) with sprouting axons. Scale bar = 20µm in A, 10 µm in B1,B2,B3.

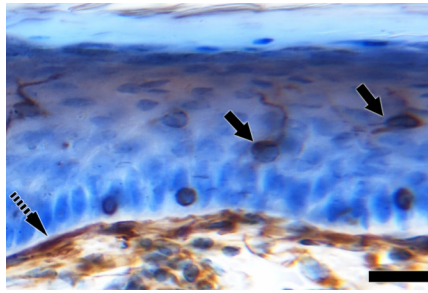


**Figure 4. Light microscopic findings of Schwann cells in post-axotomy sections immunostained for s100**

At Day 28 post-axotomy, prominent s100 immunopositive dermal Schwann cells (hatched arrow) and Langerhans cells in epidermis (arrow) were detected but cells morphologically consistent with epidermal Schwann cells that expressed s100 were not observed.

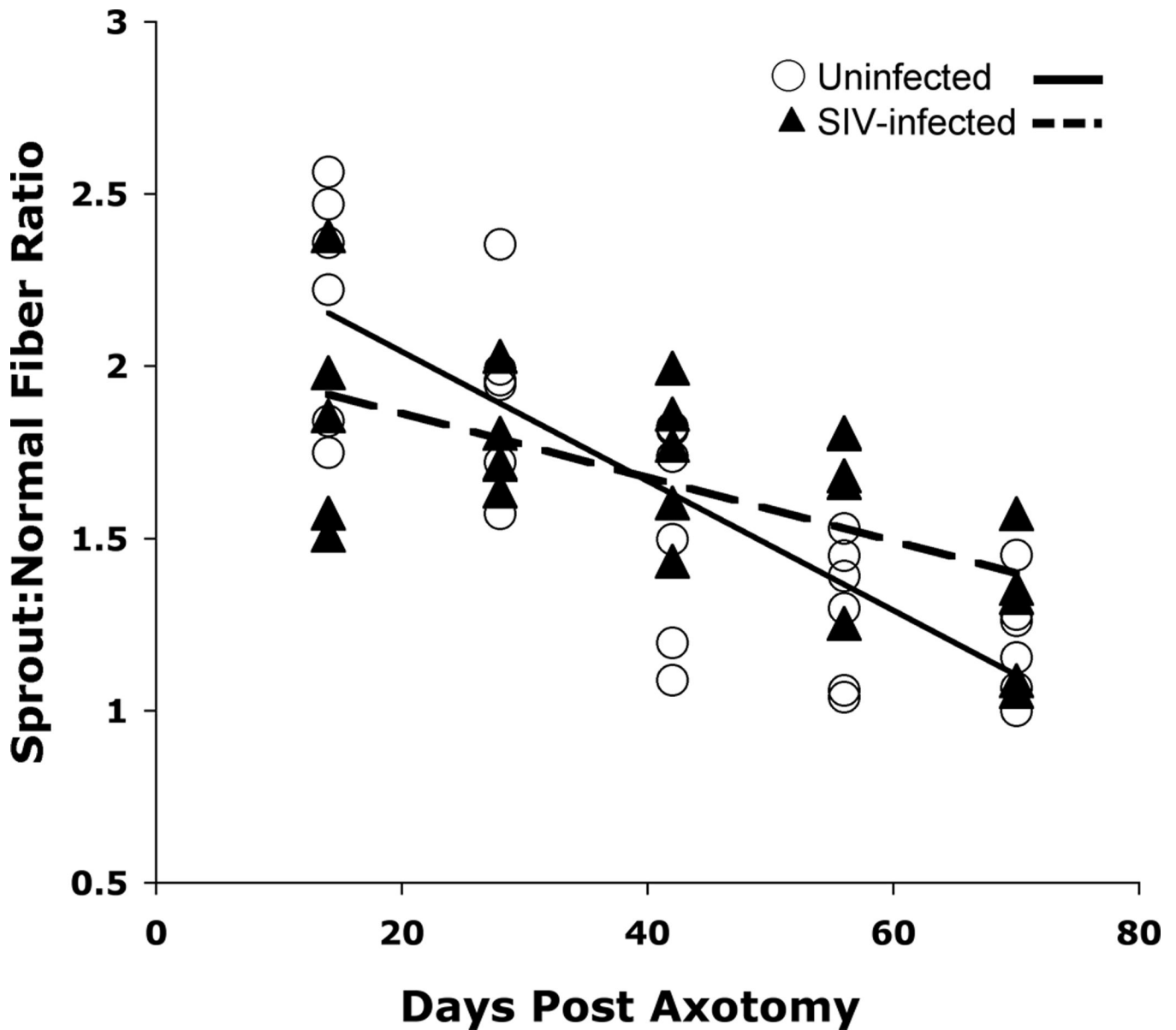


**Figure 5. SIV infection alters epidermal nerve fiber length post-axotomy**

In contrast with uninfected macaques (circles, solid line), SIV-infected macaques (triangles, dashed line) had lower mean ratios of collateral sprout length (S) to normal nerve fiber length (N) at 14 day post-axotomy. Over time, the change in S: N ratio in SIV-infected macaques was significantly less than the S: N ratio in control macaques ( $p = 0.015$ , repeated measures regression) indicating that SIV-infection delayed epidermal fiber regeneration following axotomy.

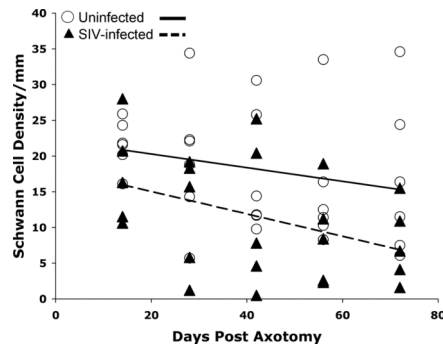


**Figure 6. SIV infection alters epidermal Schwann cell density post-axotomy**

At every time point post-axotomy, the group of SIV-infected macaques (triangles, dashed line) consistently had lower mean Schwann cell density measurements in the epidermis than uninfected macaques (circles, solid line) however these differences were not statistically significant ( $p > 0.05$ , t-test). In both infected and control animal groups, Schwann cell process density was highest at the earliest time points post-axotomy and then declined at a similar rate for both groups over time ( $p = 0.18$ ; repeated measures regression).

Table 1

## Primary antibodies

Antibody	Source	Catalog No. (Lot No.)	Immunogen	Type/Format	Dilution
Anti-Protein Gene Product (PGP9.5)	Chemicon	AB1761 (0701049670A)	Recombinant human Ubiquitin C-terminal Hydrolase (UCH-L1)	Polyclonal rabbit serum	1:2000
Anti- Nerve Growth Factor Receptor p75	Chemicon	MAB5386 (2406089)	Human melanoma cell line WM245	Monoclonal purified immunoglobulin (ME20.4)	1:500
Anti-S-100 ( $\beta$ -subunit)	Sigma	S2532 (096K4868)	Purified bovine brain S-100b	Mouse ascites fluid	1:500